Scaling of 3D solitary waves observed by FAST and POLAR

M. Berthomier,[1,2] R. Pottelette,[1] L. Muschietti,[2] I. Roth,[2] and C. W. Carlson[2]

Received 26 August 2003; revised 29 September 2003; accepted 15 October 2003; published 20 November 2003.

[1] FAST observations of Debye-length-scale potential structures are ubiquitous in the auroral return current region of the magnetosphere. We show that the 3D shape of these fast-moving coherent structures can be correctly reproduced with a nonlinear fluid model of a 3D electron-acoustic beam soliton. This model describes the early stage of the nonlinear beam-plasma instability which takes place on the high-potential side of an electrostatic potential ramp, where cold ionospheric electrons are accelerated up the magnetic field lines by a localized DC parallel electric field. At FAST altitudes (below 4000 km), our model predicts spheroidal potential structures, while at higher altitudes we expect the solitary waves to be elongated across the magnetic field. This altitude-dependent scaling is in agreement with observations of solitary waves performed with POLAR over a wide range of altitudes. *INDEX TERMS:* 2704 Magnetospheric Physics: Auroral phenomena (2407); 2712 Magnetospheric Physics: Electric fields (2411); 7815 Space Plasma Physics: Electrostatic structures. **Citation:** Berthomier, M., R. Pottelette, L. Muschietti, I. Roth, and C. W. Carlson, Scaling of 3D solitary waves observed by FAST and POLAR, *Geophys. Res. Lett.*, *30*(22), 2148, doi:10.1029/2003GL018491, 2003.

1. Introduction

[2] Observations by the Fast Auroral SnapshoT (FAST) satellite [*Carlson et al.*, 1998a] have shown that solitary structures and energetic upgoing electrons are ubiquitous in the return current region of the auroral magnetosphere [*Ergun et al.*, 1998]. These small-scale structures are possibly responsible for the generation of electrostatic whistler waves [*Berthomier et al.*, 2002]. They carry an energy up to $\sim$1% of the thermal energy, which is typical of strong turbulence. They are associated with strong ion heating and ion outflow and therefore they seem to play a significant role in ionosphere-magnetosphere coupling.

[3] Figure 1 displays the typical electric field signature of the solitary structures observed by FAST at 3100 km altitude, 21 MLT, and 69° ILAT [*Ergun et al.*, 1998]. The parallel and perpendicular electric fields, $E_{\|}$ and $E_{\perp}$, take the form of bipolar and quasi-monopolar spikes, respectively. They correspond to Debye-length-scale positive potential structures moving upwards at a few thousand km/s along the magnetic field **B**. These structures are similar to the electrostatic potential spikes observed by the POLAR spacecraft at higher altitude in the polar cap and in the plasma sheet boundary layer [*Mozer et al.*, 1997; *Cattell et al.*, 1999]. Using a statistical analysis of the ratio $E_{\perp}/E_{\|}$ for structures detected by POLAR over a wide range of altitude, *Franz et al.* [2000] have shown that the ratio of their perpendicular to parallel elongation relative to the magnetic field, $L_{\perp}/L_{\|}$, varies as $\sqrt{1+\omega_{pe}^2/\Omega_{ce}^2}$ where ω_{pe} and Ω_{ce} are the electron plasma frequency and gyrofrequency, respectively.

[4] In this paper, we present the first model of a 3D electrostatic structure which self-consistently accounts for this scaling. At FAST altitudes, where $\omega_{pe}/\Omega_{ce} \ll 1$, the model, in agreement with the observations, predicts spheroidal structures, while at higher altitudes it predicts the solitary waves to be elongated across the magnetic field.

2. Theory

[5] In order to construct our model, we first need to consider realistic electron distribution functions. Typical electron distribution functions observed in association with the solitary waves have little thermal spread across **B** and form a plateaued distribution along **B** [*Carlson et al.*, 1998b]. These distributions have been strongly thermalized and they probably result from the evolution of a two-stream instability: in the current-carrying auroral plasma, a localized density inhomogeneity may indeed induce the formation of an electrostatic potential ramp from which emerges an electron beam that interacts with the non-drifting electrons of higher temperature which stagnate upstream (i.e. on the high-potential side of the ramp) [*Newman et al.*, 2001]. Recently confirmed by high-time resolution FAST observations [*Ergun et al.*, 2001], this scenario implies the existence of a localized parallel electric field in the auroral plasma. Solitary waves are formed upstream of this double-layer.

[6] In the following, we describe only the first stage of the nonlinear evolution of this system, in the immediate vicinity of the potential ramp: we want to answer the question of whether solitary structures have a 3D preferential shape from the very beginning of their nonlinear evolution. All physical quantities are considered as only slightly different from their equilibrium values, and strong nonlinear effects, like particle trapping, are neglected. However, trapped electrons play an important role for large-amplitude solitary waves which have been previously modeled as 1D electron holes [e.g., *Muschietti et al.*, 1999]. Here we adopt a fluid point of view and write the following set of equations for the two electron populations:

$$\frac{\partial n_i}{\partial t} + \nabla \cdot (n_i \mathbf{v}_i) = 0 \quad (1)$$

$$\frac{\partial \mathbf{v}_i}{\partial t} + \mathbf{v}_i \cdot \nabla \mathbf{v}_i = \frac{e}{m_e}\nabla\phi - \frac{\nabla \cdot \mathbf{P}_i}{n_i m_e} + \Omega_{ce}\mathbf{v}_i \times \mathbf{z} \quad (2)$$

[1]Centre d'étude des Environnements Terrestre et Planétaires, IPSL, Saint-Maur, France.
[2]Space Sciences Lab, University of California, Berkeley, California, USA.

0094-8276/03/2003GL018491$05.00

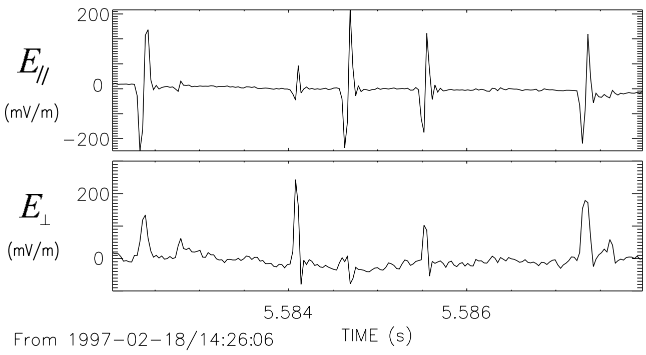

Figure 1. Parallel and perpendicular electric field signature of a series of solitary waves observed by FAST in the downward current auroral region.

$$\nabla^2 \phi = \frac{e}{\varepsilon_0}(n_s + n_b - n_0) \tag{3}$$

where n is the density, $\mathbf{v}$ the velocity, ϕ the electrostatic potential, $\mathbf{P}$ the pressure tensor, and the subscript $i = s$, or b refers to stationary, and beam electrons. The magnetic field $\mathbf{B}$ is oriented along -$\mathbf{z}$, and -e and m_e are the electron charge and mass, respectively. We close the hierarchy of fluid equations by assuming that the plasma behaves as an ideal gas with an anisotropic equation of state for the pressure. The pressure tensor splits into perpendicular and parallel components, $p_{\perp,\parallel} = nk_BT_{\perp,\parallel}$, and a polytropic law relates temperature to density variations, $T_{\perp,\parallel} = T_{\perp 0,\parallel 0}\,(n/n_0)^{\gamma\perp,\parallel-1}$ where $\gamma_{\perp,\parallel}$ are perpendicular and parallel polytropic indices which are *a priori* distinct for the two electron populations. The subscript 0 refers to undisturbed quantities. We will show in Section 3 how polytropic indices can be determined. Due to the high speed of the solitary wave compared to the ion-thermal and ion-acoustic velocities, ions are assumed to form a homogeneous neutralizing background in Poisson equation (3), with density n_0.

[7] We first identify the linear wave modes of this system by linearizing (1)–(3) with the ansatz $\phi \propto \exp(i\Phi_W)$ where $\Phi_W = \mathbf{k}\cdot\mathbf{r} - \omega t$ is the wave phase. For illustrative purposes we first consider the case with a cold beam ($T_b = 0$) and hot isotropic stationary plasma, for which $\omega/k_\parallel \ll v_s$ where $v_s^2 = \gamma_s k_B T_s/m_e$ is the stationary electron isotropic thermal velocity. From the linearization of (1)–(3), we get

$$(\omega - k_\parallel u_d)^2 = \frac{k_\parallel^2 v_{ea}^2}{1 + k^2\lambda_{Ds}^2}\left\{1 + \frac{k_\perp^2}{k_\parallel^2}\frac{(\omega - k_\parallel u_d)^2}{\left[(\omega - k_\parallel u_d)^2 - \Omega_{ce}^2\right]}\right\} \tag{4}$$

where u_d is the beam velocity and $v_{ea} = \lambda_{Ds}\omega_{pb}$ is the electron-acoustic velocity, with λ_{Ds} being the stationary electron Debye length and ω_{pb} the beam plasma frequency. In a strongly magnetized plasma with $(\omega - k_\parallel u_d) \ll \Omega_{ce}$, (4) reduces to

$$(\omega - k_\parallel u_d)^2 = \frac{k_\parallel^2 v_{ea}^2}{1 + k^2\lambda_{Ds}^2 + k_\perp^2\rho^2} \tag{5}$$

where $\rho = v_{ea}/\Omega_{ce}$ is the electron-acoustic gyroradius. For obliquely propagating weakly dispersive waves, we have $k\lambda_{Ds} \ll 1$ and $k_\perp\rho \ll 1$ and the dispersion relation takes the form $\omega \sim k_\parallel u_d - k_\parallel v_{ea}\,(1 - k^2\lambda_{Ds}^2/2 - k_\perp^2\rho^2/2)$. In a more general case with non-zero beam temperature and arbitrary wave phase velocity relative to v_s, a similar expression can be obtained:

$$\omega \sim k_\parallel u_d - k_\parallel V_{EA}\left(1 - k^2\lambda_D^2/2 - k_\perp^2\rho_L^2/2\right) \tag{6}$$

where V_{EA}, λ_D, and ρ_L are an effective electron-acoustic velocity, Debye length, and electron-acoustic gyroradius, respectively. We further define $V = u_d - V_{EA}$ as the long-wavelength limit of the parallel wave phase velocity.

[8] We aim to expand all physical quantities around these linear solutions in the reference frame of the linear wave. In the weakly dispersive limit, we define a small parameter ε such that $k^2 = \varepsilon K^2$ with K of the order of typical length scales of the plasma like λ_D or ρ_L. From (6), the wave phase becomes

$$\begin{aligned}\Phi_W = \mathbf{K}_\perp \cdot \left[\varepsilon^{1/2}\mathbf{r}_\perp\right] + K_\parallel\left[\varepsilon^{1/2}\left(r_\parallel - Vt\right)\right] \\ - K_\parallel V_{EA}\left(K^2\lambda_D^2 + K_\perp^2\rho_L^2\right)\left[\varepsilon^{3/2}t\right]/2\end{aligned} \tag{7}$$

and we conclude that we need to stretch space and time variables according to

$$[\zeta, \eta, \xi, \tau] = \left[\varepsilon^{1/2}x, \varepsilon^{1/2}y, \varepsilon^{1/2}(z - Vt), \varepsilon^{3/2}t\right] \tag{8}$$

in order to study the nonlinear waves in the reference frame of the linear solutions of (1)–(3). This implies that

$$\left(\frac{\partial}{\partial x}, \frac{\partial}{\partial y}, \frac{\partial}{\partial z}\right) = \varepsilon^{1/2}\left(\frac{\partial}{\partial \zeta}, \frac{\partial}{\partial \eta}, \frac{\partial}{\partial \xi}\right) \tag{9}$$

$$\frac{\partial}{\partial t} = -V\varepsilon^{1/2}\frac{\partial}{\partial \xi} + \varepsilon^{3/2}\frac{\partial}{\partial \tau} \tag{10}$$

[9] Using the reductive perturbation method [*Washimi and Taniuti*, 1966] adapted for obliquely propagating waves by *Laedke and Spatschek* [1982], we expand all quantities in power series of ε

$$n_{s,b} = n_{s0,b0} + \varepsilon n_{s,b}^{(1)} + \varepsilon^2 n_{s,b}^{(2)} + \ldots \tag{11}$$

$$v_{s\xi} = 0 + \varepsilon v_{s\xi}^{(1)} + \varepsilon^2 v_{s\xi}^{(2)} + \ldots \tag{12}$$

$$v_{b\xi} = u_d + \varepsilon v_{b\xi}^{(1)} + \varepsilon^2 v_{b\xi}^{(2)} + \ldots \tag{13}$$

$$\phi = 0 + \varepsilon\phi^{(1)} + \varepsilon^2\phi^{(2)} + \ldots \tag{14}$$

$$v_{s\zeta,b\zeta} = 0 + \varepsilon^{3/2} v_{s\zeta,b\zeta}^{(1)} + \varepsilon^2 v_{s\zeta,b\zeta}^{(2)} + \ldots \tag{15}$$

$$v_{s\eta,b\eta} = 0 + \varepsilon^{3/2} v_{s\eta,b\eta}^{(1)} + \varepsilon^2 v_{s\eta,b\eta}^{(2)} + \ldots \tag{16}$$

where undisturbed densities, $n_{s0,b0}$, have been introduced. Note that the specific expansion for the perpendicular velocity in (15) and (16) will be justified later on.

[10] Solving (1) and (3) together with the parallel component of (2) to order 1 and 3/2 in ε in terms of the new variables (ζ, η, ξ, τ), it can be easily shown that V must be equal to the parallel wave phase velocity of the linear mode. Therefore V is a known function of the plasma parameters. To order 3/2 in ε, the perpendicular component of (2) gives

$$\begin{bmatrix} v_{s\eta}^{(1)} \\ -v_{s\zeta}^{(1)} \end{bmatrix} = \frac{-e}{m_e\Omega_{ce}}\nabla_\perp\phi^{(1)} + \frac{\gamma_{\perp s}k_B T_{\perp s0}}{m_e\Omega_{ce}}\frac{n_s^{(\gamma_{\perp s}-2)}\nabla_\perp n_s^{(1)}}{n_{s0}^{(\gamma_{\perp s}-1)}} \quad (17)$$

A similar equation is obtained for the electron beam. The first term on the right hand side of (17) is the "$\mathbf{E} \times \mathbf{B}$" drift while the second one is the diamagnetic drift due to the electron pressure gradient. This result makes sense as long as the drift approximation is valid, i.e. at low frequency compared to the electron gyrofrequency Ω_{ce}. It is a direct consequence of the specific choice we made for the first term of the perpendicular velocity expansion in power series of ε, given by (15) and (16).

[11] To second order in ε, (2) reduces to

$$\begin{bmatrix} v_{s\eta}^{(2)} \\ v_{s\zeta}^{(2)} \end{bmatrix} = \frac{V}{\Omega_{ce}}\frac{\partial}{\partial\xi}\begin{bmatrix} -v_{s\zeta}^{(1)} \\ +v_{s\eta}^{(1)} \end{bmatrix} \quad (18)$$

For the electron beam, a similar equation is derived with V replaced by $V - u_d$ in (18). The right-hand term of (18) comes from the convective part of the time derivative given by (10) and, by looking at (17), we can interpret the second order perpendicular velocity as the polarization drift. This physically reasonable result justifies the specific power of ε considered in the second term of (15) and (16). Another choice in these expansions would be required for the description of a different ordering of the characteristic frequencies of the plasma.

[12] Finally, to order 5/2 in ε, we obtain from (1)–(3) a system of equations which relates second and first-order quantities and which constrains the dynamical evolution of the system to first order in ε. After lengthy but straightforward calculations, we have obtained the following evolution equation for the potential perturbation $\phi^{(1)}$

$$A\frac{\partial\phi^{(1)}}{\partial\tau} + B\phi^{(1)}\frac{\partial\phi^{(1)}}{\partial\xi} + \frac{\partial}{\partial\xi}\left[(C+1)\nabla_\perp^2\phi^{(1)} + \nabla_\parallel^2\phi^{(1)}\right] = 0 \quad (19)$$

where for convenience, space, time, and energy have been normalized to λ_{Ds}, ω_{pb}^{-1}, and $k_B T_{\parallel s0}$, respectively, and where

$$A = \frac{2V}{\alpha\left(\gamma_{\parallel s}/\alpha - V^2\right)^2} + \frac{2(V-u_d)}{\left[\gamma_{\parallel b}\theta/\alpha - (V-u_d)^2\right]^2}$$

$$B = 3\left\{\frac{V^2 + f\left(\gamma_{\parallel s},\alpha\right)}{\alpha^2\left(\gamma_{\parallel s}/\alpha - V^2\right)^3} + \frac{(V-u_d)^2 + f\left(\gamma_{\parallel b},\alpha\right)\theta}{\alpha\left[\gamma_{\parallel b}\theta/\alpha - (V-u_d)^2\right]^3}\right\}$$

$$C = \frac{\alpha(V-u_d)^4\left[1 + \left(\tilde{\gamma}_{\perp b} - \gamma_{\parallel b}\right)\theta/\alpha(V-u_d)^2\right]}{\Gamma^2\left[\gamma_{\parallel b}\theta/\alpha - (V-u_d)^2\right]^2} + \frac{V^4\left[1 + \left(\tilde{\gamma}_{\perp s} - \gamma_{\parallel s}\right)/\alpha V^2\right]}{\Gamma^2\left(\gamma_{\parallel s}/\alpha - V^2\right)^2} \quad (20)$$

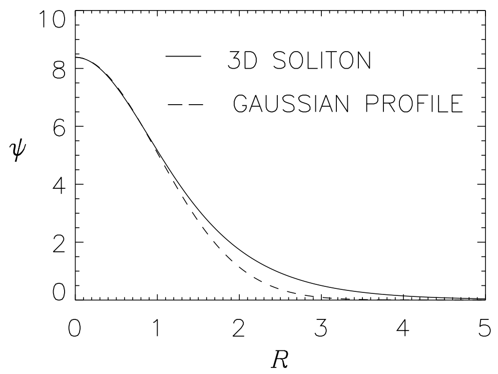

Figure 2. Potential profile of a 3D solitary wave as a function of R, the distance from its center in a stretched coordinate system moving along **B**. The dashed line is a gaussian fit to the 3D soliton model.

with (α, θ) = (n_{b0}/n_{s0}, $T_{\parallel b0}/T_{\parallel s0}$), $\Gamma = \Omega_{ce}/\omega_{ps}$, $f(\gamma_\parallel, \alpha) = \gamma_\parallel(\gamma_\parallel - 2)/(3\alpha)$, and $\tilde{\gamma}_\perp = \gamma_\perp(T_{\perp 0}/T_{\parallel 0})$. Note that velocities V and u_d are hereafter normalized to v_{ea}. Our evolution equation is of the form of the Zakharov-Kuznetsov equation derived for ion-acoustic perturbations in a simple two component plasma [*Zakharov and Kuznetsov*, 1974].

[13] For purely 1D perturbations, (19) reduces to the well-known Korteweg-de Vries equation which admits stationary localized solutions in the form of electron-acoustic solitons [*Dubouloz et al.*, 1991] associated with either a positive or a negative potential profile [*Berthomier et al.*, 2000]. In the 3D case, the form of (19) suggests a change in coordinates such that $(X, Y) = (\zeta, \eta)/\sqrt{C(V)+1}$ and $Z = \xi$. This allows us to unify the last two terms of (19) into a single term $\partial\,[\nabla^2\phi^{(1)}]/\partial Z$. Looking for stationary nonlinear perturbations which move along **B** at a velocity slightly different from the parallel phase velocity of the linear modes, we perform a second galilean transformation $(\bar{x}, \bar{y}, \bar{z}, \bar{t}) = (X, Y, Z - u\tau, \tau)$ and we impose that $\partial/\partial\bar{t} = 0$. In this new reference frame (19) can be integrated along the **z** axis, with the boundary condition $\phi^{(1)} \to 0$ when $\bar{z} \to 0$, and leads to

$$-A(V)u\phi^{(1)} + \frac{1}{2}B(V)\left[\phi^{(1)}\right]^2 + \nabla^2\left[\phi^{(1)}\right] = 0 \quad (21)$$

where the Laplacian operator ∇^2 acts on $\bar{x}$, $\bar{y}$, and $\bar{z}$. The highly symmetric form of (21) suggests looking for spherically symmetric solutions of this equation. We define R as the distance from the center of the coordinate system:

$$R = \sqrt{A(V)u(\bar{x}^2 + \bar{y}^2 + \bar{z}^2)} \quad (22)$$

and we normalize the potential $\psi = \phi^{(1)}B(V)/[A(V)u]$. The solitary wave solutions of the problem satisfy

$$-\psi + \frac{1}{2}\psi^2 + \frac{1}{R}\frac{d^2}{dR^2}(R\psi) = 0 \quad (23)$$

There is a unique localized solution ψ to (23) and it is given in Figure 2 as a function of the normalized radial distance R. A gaussian potential profile $\psi = \psi_0 \exp(-R^2/2)$ is a reasonably good fit to the 3D soliton solution, which is

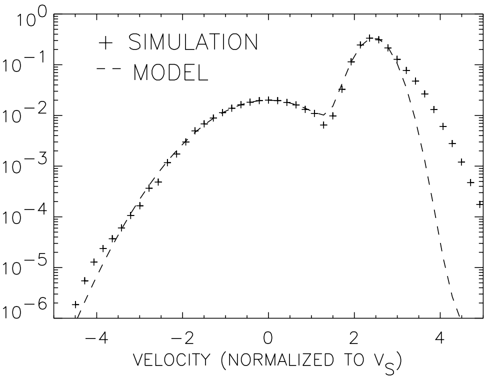

Figure 3. Electron distribution function obtained by *Newman et al.* [2001] upstream (i.e. on the high-potential side) of the potential ramp seeded by a neutral density inhomogeneity in a 1D current-carrying plasma. Our model includes stationary (non-drifting) and beam maxwellian populations.

consistent with FAST and POLAR observations of 3D solitary waves. We stress the fact that the solution we found is not spherically symmetric in the plasma reference frame, i.e. in the original coordinate system (x, y, z). Instead, it is an ellipsoid with a ratio between its perpendicular and parallel axes given by $L_\perp/L_\parallel = \sqrt{C(V)+1}$.

3. Application to FAST Observations

[14] Typical plasma parameters have been used in order to apply this model to FAST observations of 3D solitary waves in the auroral return current region. Figure 3 displays the electron distribution function observed upstream of the electrostatic potential ramp in the simulation of *Newman et al.* [2001]. The simulation uses normalized plasma parameters which are consistent with FAST observations. We expect similar beam-plasma systems to exist at POLAR altitudes. Velocity is normalized to $(k_B T_{\parallel s0}/m_e)^{1/2}$ in the simulation. A good fit of these numerical data is obtained from the superposition of two maxwellian distributions which represents the beam and stationary populations introduced in Section 2. The fit gives $\alpha = 7$, $\theta = 1/8$, and $u_d \sim 0.93$. Recall that velocities are normalized to the electron-acoustic velocity v_{ea} in our model. Perpendicular polytropic indices, which cannot be determined from the 1D simulation, are set to $\gamma_{\perp s,b} = 2$, corresponding to the adiabatic isotropic 2D case.

[15] At this point we need a method to determine the parallel polytropic indices relative to each electron population. For this purpose we will now require that the parallel phase velocity V of the fluid electron-acoustic beam mode reproduces the phase velocity obtained from a numerical analysis of the kinetic dispersion relation of this mode. Soliton models, which do not include Landau damping, are relevant when the growth rate of the corresponding kinetic linear modes is small. Therefore, our fluid model must predict the correct phase velocity of the electron-acoustic beam mode at small values of the growth rate. It turns out that the growth rate is close to zero for $V \sim 0.43$ which corresponds to $\sim 1.13\ (k_B T_{\parallel s0}/m_e)^{1/2}$ in the normalization of Figure 3. This is the fluid wave phase velocity we get for $\gamma_{\parallel s} = 1.5$ and $\gamma_{\parallel b} = 3$. This result makes sense since beam electrons behave adiabatically at $V \sim 0.43$ while stationary electrons are neither adiabatic ($\gamma_{\parallel s} = 3$) nor isothermal ($\gamma_{\parallel s} = 1$).

[16] With these parameters, we found that the coefficients $A(V)$, $B(V)$, and $C(V)$ in (20) are positive. This means that 3D electron-acoustic solitons can exist in this beam-plasma system. They are Debye-length-scale positive potential structures which propagate at velocity close to the electron-acoustic velocity along **B** (a few thousand km/s typically). This result does not depend strongly on the perpendicular electron temperature. The 3D scaling of these solitons is determined by the coefficient $C(V)$ given in (20). In the cold beam, hot stationary plasma case for instance, it turns out that $C(V) = \rho^2/\lambda_{Ds}^2$, where the electron-acoustic gyroradius ρ, and the Debye length λ_{Ds} have been introduced in the dispersion relation of the linear mode described in Section 2. In a simple electron-ion plasma without a beam, we would have $\rho_L/\lambda_D = \omega_{ps}/\Omega_{ce}$. In other words, in the general case the ratio $L_\perp/L_\parallel = \sqrt{1+\rho_L^2/\lambda_D^2}$ is equivalent to $\sqrt{1+\omega_p^2/\Omega_{ce}^2}$ where ω_p is the effective plasma frequency. A parametric study of our model shows that the beam-to-stationary density and parallel temperature ratios determine the existence of well-behaved soliton solutions, while their 3D scaling essentially depends on the value of the absolute electron density and magnetic field strength. With $\Omega_{ce}/\omega_p > 10$ at FAST altitudes (below 4000 km), $C(V) \ll 1$ and the solitons are Debye-length-scale spheres of positive potential. As it has been inferred from POLAR observations of solitary structures [*Franz et al.*, 2000], at higher altitudes, the shape of the 3D solitons becomes more oblate across **B** since plasma magnetization decreases with altitude. Note that we have taken the strong magnetization limit in our perturbative approach. Consequently our result only gives the variation to first order in ω/Ω_{ce} of $L_\perp/L_\parallel$. As noted by *Franz et al.* [2000], this condition is approximatively equivalent to $\Omega_{ce}/\omega_p > 0.3$. Using intuitive arguments based on gyrokinetic theory, these authors came to the same conclusion that the specific scaling of 3D solitary waves is a direct consequence of the differential dispersion of high-frequency electrostatic modes in parallel and perpendicular directions, which is clearly established by (19).

4. Conclusion

[17] We have shown that small-amplitude Debye-length-scale positive potential structures described as 3D electron-acoustic beam solitons can form in the current-carrying auroral plasma. The role of particle drifts across the magnetic field is essential to the soliton model. This result is in agreement with the description of 3D electron holes recently developed by [*Muschietti et al.*, 2002]. In the later model, trapped electrons are shown to perform an azimuthal and quasi-periodic motion across **B** due to the "**E** × **B**" drift associated with the potential structure. Our fluid model is also consistent with the observed altitude distribution of the ratio of the perpendicular to parallel scale of the solitary waves. This study suggests that large amplitude solitary structures observed by FAST and POLAR at different altitudes evolve from small amplitude electron-acoustic solitons and are essentially 3D from the very beginning of their evolution.

[18] **Acknowledgments.** This research is part of the France-Berkeley program. We are grateful to D. L. Newman for providing us with the electron distribution observed in his simulations. This work was supported by NASA grant NAG5-3596.

References

Berthomier, M., R. Pottelette, M. Malingre, and Y. Khotyaintsev, Electron-acoustic solitons in an electron-beam plasma system, *Phys. Plasmas*, *7*, 2987–2994, 2000.

Berthomier, M., L. Muschietti, J. W. Bonnell, I. Roth, and C. W. Carlson, Interaction between electrostatic whistlers and electron holes in the auroral region, *J. Geophys. Res.*, *107*, 1463, doi:10.1029/2002JA009303, 2002.

Carlson, C. W., R. F. Pfaff, and J. G. Watzin, The Fast Auroral SnapshoT (FAST) mission, *Geophys. Res. Lett.*, *25*, 2013–2016, 1998a.

Carlson, C. W., et al., FAST observations in the downward auroral current region: Energetic upgoing electron beams, parallel potential drops, and ion heating, *Geophys. Res. Lett.*, *25*, 2017–2020, 1998b.

Cattell, C. A., et al., Comparisons of Polar satellite observations of solitary wave velocities in the plasma sheet boundary and the high-altitude cusp to those in the auroral zone, *Geophys. Res. Lett.*, *26*, 425–428, 1999.

Dubouloz, N., R. Pottelette, M. Malingre, and R. A. Treumann, Generation of broadband electrostatic noise by electron-acoustic solitons, *Geophys. Res. Lett.*, *18*, 155–158, 1991.

Ergun, R. E., et al., Direct observation of localized parallel electric fields in a space plasma, *Phys. Rev. Lett.*, *87*, 045,003/1–4, 2001.

Ergun, R. E., et al., Fast satellite observations of large-amplitude solitary structures, *Geophys. Res. Lett.*, *25*, 2041–2044, 1998.

Franz, J. R., P. M. Kintner, C. E. Seyler, J. S. Pickett, and J. D. Scudder, On the perpendicular scale of electron phase-space hole, *Geophys. Res. Lett.*, *27*, 169–172, 2000.

Laedke, E. W., and K. H. Spatschek, Nonlinear ion-acoustic waves in weak magnetic fields, *Phys. Fluids*, *25*, 985–989, 1982.

Mozer, F. S., R. Ergun, M. Temerin, C. Cattell, J. Dombeck, and J. Wygant, New features of time domain electric-field structures in the auroral acceleration region, *Phys. Rev. Lett.*, *79*, 1281–1284, 1997.

Muschietti, L., R. E. Ergun, I. Roth, and C. W. Carlson, Phase-space electron holes along magnetic field lines, *Geophys. Res. Lett.*, *26*, 1093–1096, 1999.

Muschietti, L., I. Roth, C. W. Carlson, and M. Berthomier, Modeling stretched solitary waves along magnetic field lines, *Nonlinear Processes in Geophysics*, *9*, 101–109, 2002.

Newman, D. L., M. V. Goldman, R. E. Ergun, and A. Mangeney, Formation of a double layers and electron holes in a current-driven space plasma, *Phys. Rev. Lett.*, *87*, 255,001/1–4, 2001.

Washimi, H., and T. Taniuti, Propagation of ion-acoustic solitary waves of small amplitude, *Phys. Rev. Lett.*, *17*, 996–998, 1966.

Zakharov, V. E., and E. A. Kuznetsov, Three-dimensional solitons, *Soviet Phys. JETP*, *39*, 285–286, 1974.

M. Berthomier and R. Pottelette, CETP/IPSL, Saint-Maur, 94107 Cedex, France. (mbr@cetp.ipsl.fr)

L. Muschietti, I. Roth, and C. W. Carlson, Space Sciences Lab, University of California, Berkeley, CA 94720-7450, USA.